STEM CELLS AND DEVELOPMENT
Volume 23, Number 14, 2014

DOI: 10.1089/scd.2013.0477

Functional Comparison of Human-Induced Pluripotent Stem Cell-Derived Mesenchymal Cells and Bone Marrow-Derived Mesenchymal Stromal Cells from the Same Donor

Solvig Diederichs* and Rocky S. Tuan

Mesenchymal stem cells (MSCs) have a high potential for therapeutic efficacy in treating diverse musculoskeletal injuries and cardiovascular diseases, and for ameliorating the severity of graft-versus-host and autoimmune diseases. While most of these clinical applications require substantial cell quantities, the number of MSCs that can be obtained initially from a single donor is limited. Reports on the derivation of MSC-like cells from pluripotent stem cells (PSCs) are, thus, of interest, as the infinite proliferative capacity of PSCs opens the possibility to generate large amounts of uniform batches of MSCs. However, characterization of such MSC-like cells is currently inadequate, especially with regard to the question of whether these cells are equivalent or identical to MSCs. In this study, we have derived MSC-like cells [induced PSC-derived MSC-like progenitor cells (iMPCs)] using four different methodologies from a newly established induced PSC line reprogrammed from human bone marrow stromal cells (BMSCs), and compared the iMPCs directly with the originating parental BMSCs. The iMPCs exhibited typical MSC/fibroblastic morphology and MSC-typical surface marker profile, and they were capable of differentiation in vitro along the osteogenic, chondrogenic, and adipogenic lineages. However, compared with the parental BMSCs, iMPCs displayed a unique expression pattern of mesenchymal and pluripotency genes and were less responsive to traditional BMSC differentiation protocols. We, therefore, conclude that iMPCs generated from PSCs via spontaneous differentiation represent a distinct population of cells which exhibit MSC-like characteristics.

Introduction

Mesenchymal stem cells (MSCs) have been considered a progenitor cell population for connective tissues, including bone, cartilage, and adipose. Bone marrow stromal cell (BMSC) preparations containing multipotent MSCs have, therefore, been extensively studied for their efficacy in treating diverse musculoskeletal injuries and disorders. Beyond their ability to supply progenitors that replenish or rebuild lost/damaged tissues, MSCs have been increasingly recognized for their trophic and immune regulatory activities [1,2]. These insights have stimulated a plethora of new clinical trials for indications as diverse as cardiovascular diseases, neurological disorders, as well as graft-versus-host and autoimmune diseases. Clinical translation of MSCs has been constrained by the invasiveness of tissue harvest and the limited facility to deliver substantial amounts of high-quality cells. Only a limited number of BMSCs can be obtained initially from a single donor and although the ex vivo expansion of BMSCs can be considerable, it is, nonetheless, finite. Being adult somatic cells with a limited life span, after a number of passages in culture, BMSCs undergo cellular senescence accompanied by decreasing proliferative and differentiation capability [3], which critically compromises their applicability for regenerative medicine and tissue engineering approaches. Moreover, their proliferative potential and differentiation capacity decline even more with increasing age and in patients with skeletal or metabolic diseases [4], impeding autologous applications for those patients who are especially in need of regenerative medicine. Perinatal and more primitive fetal MSC sources offer highly abundant cells with increased proliferative potential and differentiation capacity, but their autologous availability is limited [5,6].

Pluripotent stem cells (PSCs), including both embryonic stem cells (ESCs) and induced pluripotent stem cells (iPSCs),

Department of Orthopedic Surgery, Center for Cellular and Molecular Engineering, University of Pittsburgh School of Medicine, Pittsburgh, Pennsylvania.
*Current affiliation: Research Center for Experimental Orthopedics, Heidelberg University Hospital, Heidelberg, Germany.

possess unlimited proliferative capacity and have, thus, been investigated intensely for their applications in regenerative medicine. These PSCs are unique in their ability to differentiate into virtually any cell type derived from the three embryonic lineages (ie, ectoderm, mesoderm, and endoderm). However, the developmental immaturity of PSCs also renders their directed differentiation in vitro into specific tissue-forming cells—a process that requires the coordinated development of a number of well-defined intermediate cell types—particularly challenging [7]. Reports on the derivation of MSC-like cells from PSCs [8,9] are, thus, intriguing, as this approach combines the advantage of unlimited proliferative capacity of PSCs with the well-known properties of BMSCs, and might open the possibility to generate large amounts of highly uniform batches of MSCs. Using iPSCs rather than ESCs as the starting cell type offers the additional capability of developing autologous cells and tissues. The possibility to reproducibly generate readily expandable, patient-specific multipotent human MSC-like cell preparations from well-characterized iPSC lines represents a promising endeavor in the field of regenerative medicine. Moreover, the ability to derive MSCs from PSCs in vitro presents the opportunity to understand MSC derivation and development in vivo.

PSC-derived MSC-like progenitor cells (PMPCs) have been reported to be immature cells in a transitional state of development (between stem cells and terminally differentiated cells) [10]. Their restricted capacity to self-renew and differentiate should, in theory, preclude tumorigenicity, making them, therefore, attractive with regard to safety aspects and therapeutic applicability. Using a number of different approaches and ESC as well as iPSC lines, several groups have reported the derivation of cells that expressed MSC surface markers. Importantly, these cells did not show tumorigenicity when transplanted into immunodeficient mice [11,12]. However, their capability to form mesodermal tissues in vivo and even their in vitro trilineage differentiation capacity remain debatable. Although after respective induction positive results of standard lineage analyses (ie, in vitro calcification for osteogenesis, proteoglycan production for chondrogenesis, and production of lipid droplets for adipogenesis, in combination with expression of lineage marker genes) have been reported [13–16], the quality and degree of differentiation capacity of PMPCs in direct comparison with well-described BMSCs are insufficiently assessed.

An additional query is whether PMPCs are related, similar, or identical to MSCs, which is critical to assessing to what extent PMPCs will be capable of substituting for MSCs in regenerative applications. Characterization of PMPCs has been restricted by the current multitude of highly variable derivation procedures, ranging from forced differentiation of PSC colonies [17] or single cells [12] to the intermediate generation of embryoid bodies (EBs) [14], and to coculture with mesenchymal cell lines [8]. Another variable of significance is cellular epigenetic memory that is related to the individual characteristics of the parental cell line used for PMPC derivation.

With regard to a qualified comparison with BMSCs, not only PMPC diversity but also BMSC heterogeneity complicates experiments. BMSC heterogeneity is a consequence of their still incompletely known in vivo cell identity, such that the performance of individual BMSC populations is highly dependent on harvest method, age as well as medical condition and history of the donor, and the specific cell culture methods [18,19]. The very few studies so far that report a direct comparison between PMPCs and BMSCs [20,21] are hampered by the disadvantage of using PMPCs and BMSCs from different sources; thus, an unattainably high number of individual cell sources would be needed to compensate for cellular heterogeneity.

To circumvent these challenges, our strategy here was to convert in a first step a well-characterized, high-quality human BMSC population into a completely reprogrammed and stable iPSC line. These iPSCs were in a second step differentiated into PMPCs, enabling for the first time a direct side-by-side comparison with the originating BMSCs from the same donor. These PMPCs complied with the minimal criteria for defining MSCs developed by the International Society for Cellular Therapy (ISCT) [22] and recently adjusted for defining stromal cells from adipose tissue [23]. In accordance with these criteria, PMPCs expressed certain surface markers, adhered to tissue culture plastics, and exhibited a general trilineage differentiation capacity. However, in direct comparison with BMSCs from the same donor, PMPC gene expression still markedly deviated from BMSCs, and in vitro differentiation outcomes using the standard protocols specifically developed for MSCs proved far less efficient for PMPCs. Interestingly, differences between PMPCs and BMSCs were far more pronounced than variabilities between PMPC populations that had been derived by diverse protocols. Taken together, our findings showed that PMPCs, although exhibiting MSC-like characteristics, are still functionally distinct from BMSCs.

Materials and Methods

BMSC culture

Human BMSCs from one subject (age 48, male) were chosen from our established BMSC bank and used for all experiments in this study. The selection was based on a high available cell number and stable in vitro trilineage differentiation capacity (data not shown). BMSCs in our bank were harvested from femoral heads as previously described [24]. Briefly, femoral heads were obtained from patients undergoing total hip arthroplasty with Institutional Review Board (IRB) approval (University of Washington and University of Pittsburgh), and bone marrow and bone chips were harvested from the core of the trabecular bone. BMSCs were cultured as tissue culture plastic adherent cell populations with BMSC growth medium [minimum essential medium α (α-MEM) containing 10% fetal bovine serum (FBS; Life Technologies), 1× antibiotic-antimycotic (Life Technologies), and 1 ng/mL FGF-2 (Ray Biotech, Inc.)]. BMSCs were routinely validated as capable of undergoing osteogenic, chondrogenic, and adipogenic differentiation using our established induction protocols [25, data not shown] and banked at passage 1. All experiments were performed with passage 3–5 cells.

iPSC culture

From the selected BMSC aliquots, one cryovial was thawed for reprogramming, while the remaining cryovials

were kept for a later comparison. Passage 3 BMSCs were reprogrammed to obtain M-iPSCs as previously described [26] via lentiviral overexpression of the four well-described pluripotency factors *Oct3/4*, *Sox2*, *Klf4*, and *c-Myc* [27]. Colonies that appeared were picked and expanded. From the best candidate clone, one stable cell line was established (M-iPSCs). M-iPSCs were routinely maintained on mitomycin C-inactivated mouse CF-1 embryonic fibroblasts with Primate ES Cell Medium (ReproCELL USA), supplemented with 1× antibiotic-antimycotic and 20 ng/mL FGF-2. Before experiments, M-iPSCs were transferred to BD Matrigel™ (BD Biosciences) with mTESR™1 medium (Stemcell Technologies) that was supplemented with 1× antibiotic-antimycotic for one passage.

A previously described AE-iPSC line, which originated from human amniotic epithelium [28], was kindly provided by Gerald P. Schatten (University of Pittsburgh), and used as an independent control iPSC line. AE-iPSCs were routinely maintained on BD Matrigel with mTESR™1 medium containing 1× antibiotic-antimycotic.

Verification of pluripotency

Immunofluorescence. Immunostaining was carried out with the following antibodies according to the recommendations of the manufacturer: Alexa Fluor® 647 mouse anti-human Oct3/4 (BD Biosciences), rabbit polyclonal to human Sox2 (Abcam) with Alexa Fluor® 488 chicken anti-rabbit, Alexa Fluor 488 mouse anti-human SSEA4 (BD Biosciences), Alexa Fluor 488 mouse anti-human TRA-1-60 (BD Biosciences), and Alexa Fluor® 555 mouse anti-human TRA-1-81 (BD Biosciences). Briefly, cells were seeded onto circular cover glasses that were precoated with gelatin (0.1%; Stemcell Technologies, No. 07903) for BMSCs or with BD Matrigel for iPSCs and cultured with the appropriate media until near confluency or to an optimal colony size, respectively. Cells were fixed with 4% neutral buffered formaldehyde and stored at 4°C until use. For intracellular staining, cells were permeabilized with 0.25% Triton X-100. Nonspecific binding was blocked with 1% bovine serum albumin before incubation with the (labeled) antibodies. In case of Sox2, cells were subsequently washed and incubated with a fluorescently labeled secondary antibody. For counterstaining, cells were washed and incubated with 1 μg/mL DAPI and subsequently mounted with Vecta Shield (Vector Laboratories).

Quantitative polymerase chain reaction. RNA from trypsinized cells was isolated with the Qiagen RNeasy Plus Mini kit according to the manufacturer's instructions. RNA extraction with TriZol (Life Technologies) was used for pellet cultures in chondrogenesis assays and adipogenesis assays. Only for adipogenesis assays, the extracted aqueous phase was used for RNA isolation with the Qiagen RNeasy Micro kit according to the manufacturer's instructions. Reverse transcription was done using Oligo(dT) primers and the SuperScript® III First-Strand kit (Life Technologies). Quantitative polymerase chain reaction (qPCR) was performed with Sybr® Green Master Mix (Life Technologies) with a StepOnePlus™ real-time PCR system (Life Technologies). Ct values of the genes of interest were normalized to the mean Ct values of β-actin and glyceraldehyde-3-phosphate dehydrogenase as reference (housekeeping) genes, and fold changes were calculated.

Teratoma formation. Passage 20 M-iPSCs were suspended in Matrigel and injected into testes (both sides, 3×10^6 cells in 10 μL) and flanks (both sides, 1×10^6 cells in 100 μL) of severe combined immunodeficient mice. Three out of four animals grew large testicular tumors, while no flank tumors were observed. After 7–8 weeks, mice were sacrificed; the tumors were isolated, fixed in 10% neutral buffered formalin, and embedded in paraffin; 5 μm sections were prepared, and stained with hematoxylin and eosin. All animal protocols were approved by our Institutional Animal Care and Use Committee.

Karyotyping. Passage 13 M-iPSCs were treated with ethidium bromide (0.1 μg/mL) for 45 min followed by Colcemid™ (0.1 μg/mL) treatment for 2 h before cell harvesting. After mitotic arrest, the cells were processed in accordance with standard cytogenetics laboratory procedures. Slides were prepared and trypsin-Giemsa banded.

Generation of MSC-like cells from iPSCs

MSC-like cells generated from iPSCs are termed iMPCs (iPSC-derived MSC-like progenitor cells) and were generated by the methods described next. For each differentiation method, $n = 6$ replicate experiments were performed, resulting in six replicate cell lines. The iMPCs generated from the AE-iPSCs are termed A-iMPCs and those from the M-iPSCs, M-iMPCs (Table 1).

Via EBs (iMPC-EB). Confluent iPSCs from each cell line (AE-iPS, M-iPS) were detached with Dispase (1 mg/mL; Stemcell Technologies) [29]. Large cell aggregates were broken up and re-plated with EB medium [Dulbecco's modified Eagle's medium (DMEM), 20% KnockOut™ serum replacement, 2 mM L-glutamine, 1× MEM nonessential amino acids solution (all from Life Technologies), and 0.1 mM 2-mercaptoethanol (Sigma-Aldrich, St. Louis, MO)] in suspension culture dishes. After 3 days, EBs were

Table 1. Derivation of MSC-Like Cells from Human-Induced Pluripotent Stem Cells

	Originating Cell Line		
Differentiation strategy	*M-iPS*	*AE-iPSC*	*References*
EBs	M-iMPC-EB	A-iMPC-EB	[29]
Spontaneous differentiation	M-iMPC-SD	A-iMPC-SD	[17]
Indirect BMSC coculture	M-iMPC-CC	A-iMPC-CC	
BMSC growth medium	M-iMPC-GM	A-iMPC-GM	[31]

BMSC, bone marrow stromal cell; CC, coculture; EB, embryoid body; GM, growth medium; iMPC, iPSC-derived mesenchymal stem cell-like progenitor cell; MSC, mesenchymal stem cell; SD, spontaneous differentiation.

harvested, and they were seeded onto gelatin with MSC derivation medium (DMEM, 10% FBS, 2 mM L-glutamine, 1 μM retinoic acid, and 1× antibiotic-antimycotic). After 8 days, EB outgrowth was trypsinized, filtered through a 40 μm mesh, plated onto gelatin with DMEM + 5% FBS, and incubated for 1 h. After washing twice, the remaining adherent cells were cultured with standard BMSC growth medium (see above).

Via spontaneous differentiation of iPS colonies (iMPC-SD). The intervals between medium exchanges were increased to 3–5 days [17]. After 10 days, more than 20%–50% of the cells appeared fibroblastic, and the undifferentiated portions of the colonies were removed. The remaining cells were transferred enzymatically (Dispase) to new Matrigel-coated plates with mTESR™1 medium. After 10 more days with two interim medium exchanges, the semi-differentiated parts of the colonies were removed manually. The remaining cells were trypsinized, re-seeded onto gelatin at a density of 20,000 cells/cm^2 with BMSC growth medium, and designated as passage 0.

Via indirect coculture (iMPC-CC). BMSC extracellular matrix (ECM) was prepared as previously described [30]. Briefly, passage 5 BMSCs were plated at 20,000 cells/cm^2 into six-well plates. After overnight incubation, mitosis was inhibited by Mitomycin C treatment (10 μg/mL), and the cells were incubated with BMSC medium for 3 weeks. BMSC-conditioned medium was harvested thrice a week. These conditioned media from specific culture days were cleared of cell debris by centrifugation, concentrated via ultrafiltration (Amicon Ultra-15, 3 kDa molecular weight cut-off; Merck Millipore), and reconstituted to the original volume with α-MEM. During the final 5 days of the 21-day culture, ascorbic acid (50 μM; Sigma-Aldrich) was added to the medium. On day 21, cells were removed from the ECM by incubation with 0.5% Triton X-100 containing 20 mM NH_4OH. The ECM was treated with DNase (100 U/mL; Sigma-Aldrich) and stored at 4°C until further use. For iMPC generation, partially dissociated iPSC colonies were seeded onto BMSC-derived ECM with day 0 BMSC-conditioned medium. After 2 days, the medium was exchanged to the reconstituted day 2 conditioned medium, which was repeated for subsequent medium changes. On day 24, cells were trypsinized, filtered through a 40 μm mesh, and re-seeded onto gelatin with BMSC growth medium (passage 0).

Via treatment with unconditioned BMSC growth medium (iMPC-GM). The medium of confluent iPSC cultures on Matrigel was switched to BMSC growth medium, and the cells were incubated for 7 days with two intermediate medium exchanges [31]. Subsequently, cells were trypsinized and subcultured on gelatin (P0).

iMPC characterization

Flow cytometry. Cells (passage 3 and 4 BMSCs, passage 5 iMPCs, passage 19 M-iPSCs, and passage 23 AE-iPSCs) were trypsinized, washed, and fixed with 4% buffered formaldehyde. Nonspecific binding sites were blocked with 10% normal mouse serum (Invitrogen) before incubating with the following antibodies: PE-mouse $IgG_{1,\kappa}$ anti-human CD73, FITC-mouse $IgG_{1,\kappa}$ anti-human CD90, PE-mouse $IgG_{1,\kappa}$ anti-human CD105, PE-mouse $IgG_{1,\kappa}$ anti-human CD44, PE-mouse $IgG_{1,\kappa}$ anti-human CD45, PE-mouse $IgG_{2a,\kappa}$ anti-human HLA-DR, Alexa Fluor 488-mouse IgM_{κ} anti-human TRA-1-60, and respective isotype controls (all from BD Biosciences). After further formaldehyde fixation of bound antibodies, cells were analyzed with a BD FACSAria™ II cell sorter. FACS analysis for iMPCs was carried out with a cell population pooled from all four to six replicate cell lines of the same origin and derivation method. Only for CD73, individual replicate lines were analyzed in detail. We found CD90 expressed on both iPSCs and BMSCs (Supplementary Fig. S1; Supplementary Data are available online at www.liebertpub.com/scd), which makes CD90 unsuitable as a marker for the mesenchymal phenotype. We, therefore, did not include CD90 in our detailed analysis.

Gene expression PCR array. RNA was isolated from three replicate cell lines for M-iMPC-EB, -SD, -CC, and -GM at passage 5, as well as from three independently cultivated BMSC replicates (passage 2 and 3), and M-iPSCs (passage 14 and 15), and reverse transcribed using the RT^2 First-Strand Kit (SA Biosciences), including genomic DNA elimination. PCR samples were prepared using the RT^2 SYBR Green/ROX PCR Master mix provided by the manufacturer and analyzed with the human MSC RT^2 Profiler™ PCR Array (SA Biosciences PAHS-082Z). Data analysis was based on a manually defined threshold guided by the positive PCR control included in the array and kept constant across all PCR array runs. Further analysis was carried out using the SA Biosciences web-based PCR array data analysis software (version 3.5). The data was first tested for PCR array reproducibility, reverse transcription efficiency, and genomic DNA contamination based on internal controls, and the cut-off value was set to 35 cycles. Data were normalized to the arithmetic mean of the five included reference genes (β-actin, β2-microglobulin, glyceraldehyde-3-phosphate dehydrogenase, hypoxanthine phosphoribosyltransferase 1, and ribosomal protein, large, P0). Outputs included fold changes and *P* values. Group comparisons were performed with BMSCs ($n = 3$), M-iPSCs ($n = 3$), and M-iMPCs, either all grouped together ($n = 12$) or in individual groups for the four derivation methods EB, SD, CC, and GM ($n = 3$ for each). An additional hierarchical cluster analysis for linkage between groups based on a Pearson's correlation was performed with the Ct values using SPSS for Windows 20.0 (SPSS, Inc.). All gene abbreviations are according to NCBI gene database.

iMPC differentiation

Passage 5 iMPCs ($n = 4$–6 replicate cell lines for each AE-iPSC and M-iPSC-derived iMPCs via the four described methods EB, SD, CC, and GM) and BMSCs ($n = 3$ independent replicates of the same cell line, passage 3 and 4) were subjected to trilineage differentiation in parallel experiments.

Osteogenesis. Cells were seeded at 20,000 cells/cm^2 and cultured in osteogenic medium (DMEM, 10% FBS, 1× antibiotic-antimycotic, 0.1 μM dexamethasone, 10 mM β-glycerophosphate, and 50 μg/mL ascorbate 2-phosphate) for approximately 3 weeks. Cell lysates of triplicates for each cell line on day 7 after osteogenic induction were prepared with 0.5% Triton X-100 and assayed for alkaline phosphatase (ALP) activity using the p-nitrophenyl phosphate liquid substrate system (Sigma-Aldrich). ALP enzyme

activity was normalized to DNA concentration measured with the Quant-iT™ PicoGreen® dsDNA Assay Kit (Life Technologies). Alizarin Red staining (2%, pH 4.2; Rowley Biochemical, Inc.) was performed on 4% formaldehyde-fixed cells after 3 weeks of osteogenic differentiation. Incorporated dye was solubilized with 10% cetylpyridinium chloride monohydrate and quantified spectrophotometrically based on A_{570}. Gene expression of typical osteogenic markers, including collagen type I (*COL1A1*), osteocalcin [bone γ-carboxyglutamate protein (*BGLAP*)], and bone sialoprotein 2 (*IBSP*), was analyzed via qPCR as described earlier.

Chondrogenesis. Cells were trypsinized and cultured as high-density pellets (250,000 cells per pellet) in chondrogenic medium (DMEM with sodium pyruvate, 1× antibiotic-antimycotic, 10 μg/mL ITS+, 0.1 μM dexamethasone, 40 μg/mL proline, 50 μg/mL ascorbate 2-phosphate, and 10 ng/mL TGF-β1) for 3 weeks. A total of 20 pellet cultures per cell line were prepared [3 for histological analysis, 7 for sulfated glycosaminoglycan (sGAG) quantification, and 10 for PCR]. For histological assessment, pellets were fixed in 4% buffered formaldehyde, paraffin embedded, and 5 μm sections were stained with Alcian blue (1%, pH 1.0) and counter stained with Nuclear Fast Red. Immunostaining for collagen type II was done with a mouse anti-human monoclonal antibody (MP Biomedicals) after antigen retrieval via hyaluronidase and pronase digestion, and with a biotinylated horse anti-mouse secondary antibody (Vector Laboratories). The staining signal was amplified via the Vector ABC kit and visualized with Vector VIP. GAG deposition was quantified in papain digests of pooled pellets using the 1,9-dimethylmethylene blue-based Blyscan™ assay (Biocolor Life Science Assays). The GAG content per pellet was calculated and normalized to DNA content measured with the Quant-iT PicoGreen dsDNA Assay Kit. Gene expression of typical chondrogenic markers, including collagen type II (*COL2A1*), aggrecan (*ACAN*), and cartilage oligomeric matrix protein (*COMP*), was measured via qPCR as described earlier.

Adipogenesis. Cells were seeded at a density of 20,000 cells/cm^2 and cultured in adipogenic medium (DMEM, 10% FBS, 1× antibiotic-antimycotic, 1 μM dexamethasone, 0.5 mM 3-isobutyl-1-methylxanthine, and 1 μg/mL ITS+) for 3 weeks. Lipid vesicles were histologically stained with Oil Red O after fixation with 4% buffered formaldehyde, and lipid content was determined spectrophotometrically (A_{510}) by measuring the amount of extracted dye. Gene expression of adipogenic markers, including adipocyte lipid-binding protein (*aP2*, also *FABP4*), peroxisome proliferator-activated receptor γ (*PPARG*), and lipoprotein lipase (*LPL*), was analyzed via qPCR as described earlier.

Statistical analyses

Mean values, standard deviation, and standard error of the mean were calculated. In addition, medians, first and third quartiles, maximal and minimal values, as well as outliers [1.5- to 3-fold interquartile range (IQR)] and extreme values (>3-fold IQR) were calculated for each group. For a comparison of the differentiation parameters between MSCs and iMPCs, a Kruskal–Wallis test with post hoc Mann–Whitney-U Signed-Rank Tests was conducted by comparing the 12 different iMPC groups ($n=4$–6) with the original MSCs. In addition, a comparison of all A-iMPCs as one group with all M-iMPCs grouped together was performed to assess the influence of epigenetic memory. Only significant Kruskal–Wallis tests were analyzed post hoc. A two-tailed significance value of $P<0.05$ was considered statistically significant. For the qPCR array, a Bonferroni-corrected P value of $P<5.6\times10^{-4}$ was considered statistically significant. Data analysis was performed with SPSS software.

Results

Since donor-dependent heterogeneity is a major limitation for comparing BMSCs with mesenchymal offsprings of PSCs, we generated a new iPSC line reprogrammed from human BMSCs via retroviral overexpression of the four Yamanaka factors *Oct4/Sox2/Klf4/c-Myc* [32]. The resulting M-iPSC line phenotypically resembled PSCs growing in colonies on feeder cells and expressed mRNAs and proteins that are commonly associated with pluripotency, while these markers in BMSCs were at levels far below those observed for PSCs (Fig. 1A, B). Moreover, M-iPSCs formed teratomas in vivo containing tissues of all three germ lines (Fig. 1C). Subsequently, we generated iMPCs and compared these with the remaining cryopreserved BMSCs from the same donor that were used to derive the M-iPSC line.

iMPC generation

Due to the lack of a standardized procedure for the derivation of MSC-like cells from PSCs, we used four different derivation strategies to cover the most common approaches (Table 1). Starting with either BMSC-derived M-iPSCs or a control human iPSC line (AE-iPSCs), we generated iMPCs via EBs (iMPC-EB), as well as via spontaneous differentiation of iPS colonies (iMPC-SD). In addition, we also used a mesenchymal coculture system to differentiate iPSCs into iMPCs. However, to avoid probable contamination with mesenchymal feeder cells during a direct coculture, we performed an indirect coculture where iPSCs were seeded on top of cell-free ECM derived from BMSCs and cultured with BMSC-conditioned medium (iMPC-CC). As a control, iPS colonies were also differentiated by treatment with unconditioned BMSC growth medium (iMPC-GM).

All four methods (EB, SD, CC, and GM) succeeded in establishing cell lines that had lost the typical morphology of undifferentiated iPSCs and were dominated by small cells with fibroblast morphology (Fig. 2A). However, cell morphology was not completely homogeneous, and large flat cells persisted in early passages and in few cases even through late passages. Population doubling time of iMPCs in earlier passages generally equaled that of BMSCs, and there were no significant differences between iMPCs generated from AE-iPSCs and M-iPSCs by the various iMP derivation methods (Fig. 2B). However, iMPCs ceased proliferating in earlier passages than BMSCs, and only a few random iMPC lines (A-iMPC-SD3, M-iMPC-SD4, M-iMPC-CC1, and M-iMPC-GM3) were capable of reaching high passage numbers.

In our first attempt to characterize the iMPC populations, we analyzed the surface marker profile of iMPCs in comparison with the equivalent BMSCs and iPSCs via flow cytometry. IMPCs generally had regained typical mesenchymal surface markers, while iPSCs (both M-iPSCs and

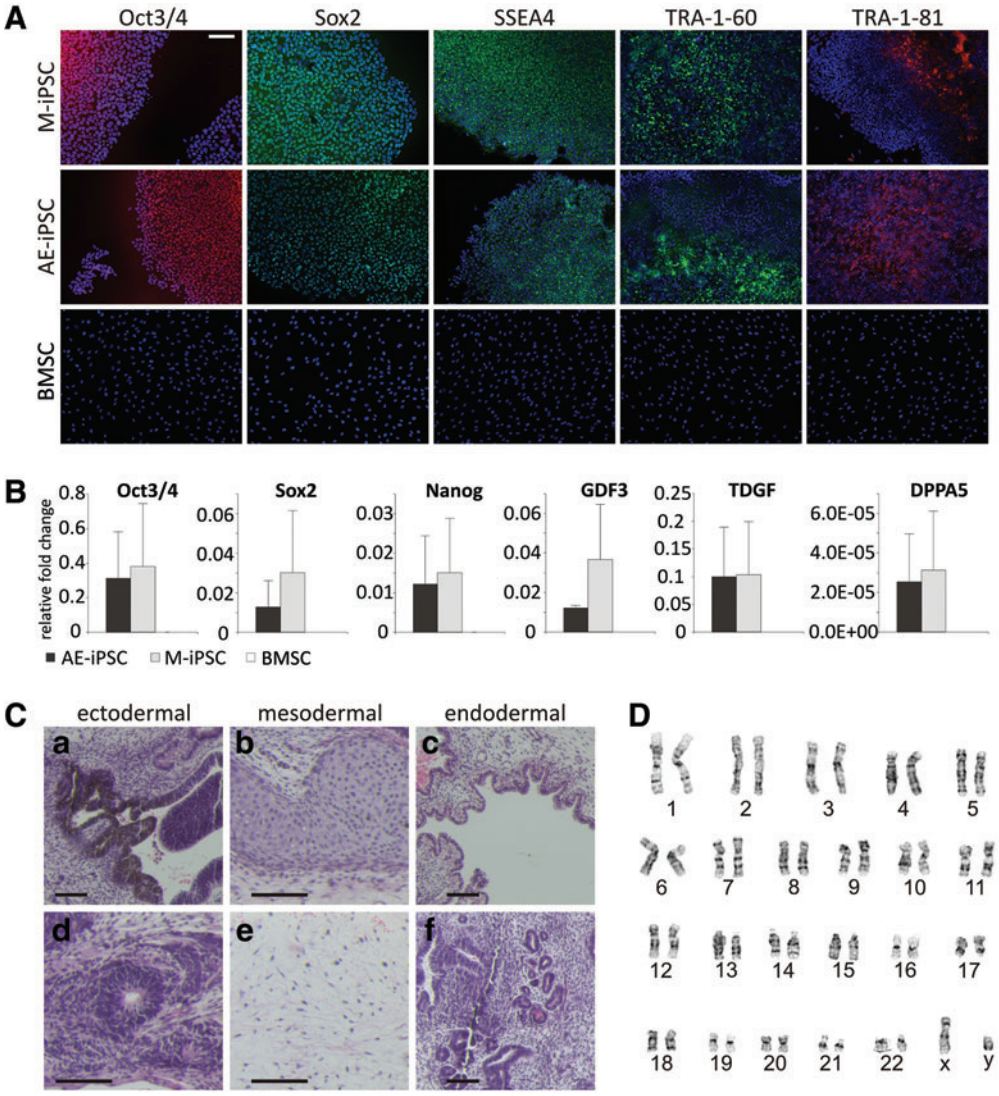

FIG. 1. Pluripotency and normal karyotype of M-iPSCs. **(A)** Immunofluorescence staining for Oct3/4, TRA-1-81 (*red*), and Sox2, SSEA4, TRA-1-60 (*green*) overlaid with DAPI staining of the nuclei (*blue*) of M-iPSCs in comparison to AE-iPSCs and BMSCs. Scale bar: 100 μm. **(B)** Comparison of levels of pluripotency-associated genes *OCT3/4*, *SOX2*, *NANOG*, *GDF3*, *TDGF*, and *DPPA5* in M-iPSCs in comparison to AE-iPSCs and BMSCs analyzed by qRT-PCR. Values of fold changes are mean ± standard deviation of three independent replicates relative to housekeeping genes. **(C)** Teratoma formation by M-iPSCs after injection into mouse testes containing tissues of all three germ layers. Hematoxylin- and Eosin-stained sections showed retinal epithelium **(a)** and neural rosettes **(d)**, cartilage **(b)** and connective tissue **(e)**, intestinal **(c),** and glandular **(f)** structures. Scale bars: 100 μm. **(D)** Normal karyotype in (male) passage 13 M-iPSCs. BMSC, bone marrow stromal cell; iPSCs, induced pluripotent stem cells. Color images available online at www.liebertpub.com/scd

AE-iPSCs) were negative for mesenchymal markers (Fig. 3 and Supplementary Fig. S2). In detail, the hyaluronic acid receptor CD44 was equally strongly expressed in iMPCs and BMSCs, independent of their origin and derivation procedure, but negative in iPSCs. Endoglin (CD105) was strongly positive in MSCs, negative in iPSCs, and tended to be positive but at a lower level in iMPCs. Here, we observed variances between the individual derivation methods, as CD105 expression tended to be higher in A-iMPCs-SD, -CC, and -GM than in the other iMPC-lines. This, however, did not correlate with the differentiation capacity (see section on iMPC differentiation) of these cell lines. For CD73, pronounced variances were evident for independent cell lines derived by different strategies. We observed subpopulations with strong positive as well as low/negative CD73 expression in the pools composed of four to six replicate cell lines (eg, for M-iMPC-SD, Fig. 3A bottom line and for A-iMPC-EB, Fig. 3B, bottom line). We, therefore, proceeded to investigate the replicate cell lines individually to examine whether heterogeneity was attributable to distinct subpopulations within individual cell lines or rather due to variances between replicates (Supplementary Fig. S3). Interestingly, we observed near homogeneous CD73 expression within each individual cell line. However, some replicate cell lines exhibited considerable variations in CD73 levels. Only M-iMPC-EBs and A-iMPC-CCs were reproducibly $CD73^{high}$. All other iMPC lines were either reproducibly $CD73^{low}$ (A-iMPC-GMs) or with CD73 levels that varied between

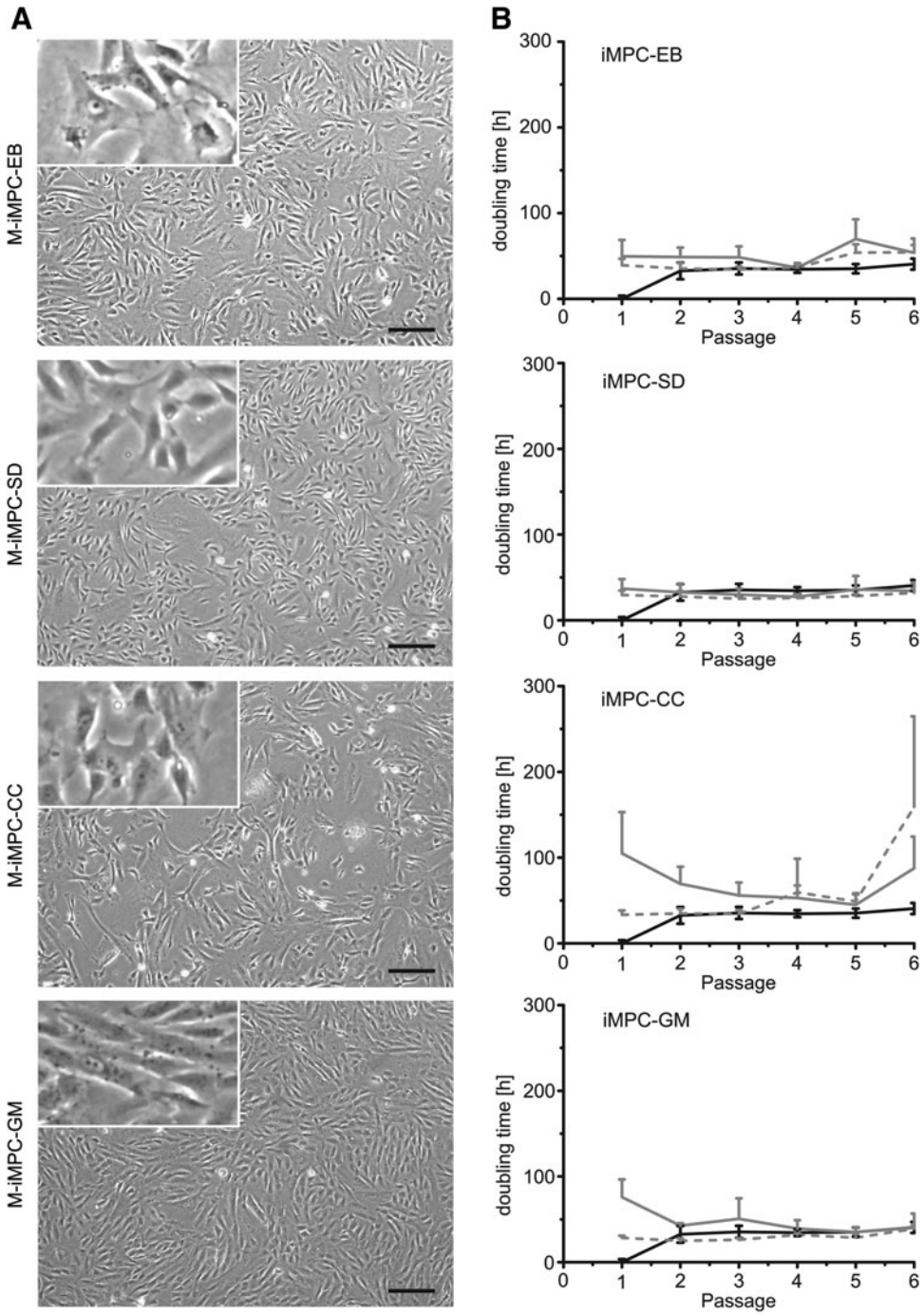

FIG. 2. Morphology and growth rates of iMPCs. **(A)** Typical cell morphology of M-iMPCs. Scale bar: 200 μm. *Insets* are fourfold magnifications. A-iMPC morphology was not markedly different from M-iMPCs. **(B)** Growth rates of BMSCs (*black line*) in comparison to M-iMPCs (*solid gray line*) and A-iMPCs (*dashed gray line*) derived using different procedures (EB, SD, CC, and GM). Values are mean ± standard deviation of four to six replicate cell lines for iMPCs and three replicates from the same donor for BMSCs. Results are presented up to passage 6. Analysis was carried out up to passage 18, with all iMPCs ceasing proliferation after passage 9 (data not shown). CC, coculture; EB, embryoid body; GM, growth medium; iMPCs, iPSC-derived mesenchymal stem cell-like progenitor cells; SD, spontaneous differentiation.

replicate cell lines. Again, this result did not correlate with the differentiation potentials of these cell lines (see section on iMPC differentiation). Inter-replicate variations of CD73 levels suggest that iMPC derivation methods yield highly variable cell populations which might be caused by the stochastic nature of the differentiation methods.

We also investigated CD45 and HLA-D/R, which are commonly used to separate BMSCs from hematopoietic stem cells (Fig. 3 and Supplementary Fig. S2). Neither CD45 nor HLA-D/R was expressed in iMPCs, BMSCs, or iPSCs. Moreover, the PSC-specific glycoprotein epitope TRA-1-60 was only expressed in iPSCs.

iMPC gene expression

To compare iMPCs with BMSCs in greater detail, specifically focusing on potential differences between the four different derivation methods, we performed PCR-based gene expression arrays using the parental BMSC line and three individual BMSC-derived M-iMPC lines for each generation method (Fig. 4). The genes profiled using the commercial human BMSC PCR array included key genes involved in maintaining stem cell pluripotency and self-renewal and also covered MSC-specific markers that distinguish them from ESCs, as well as a number of early differentiation markers.

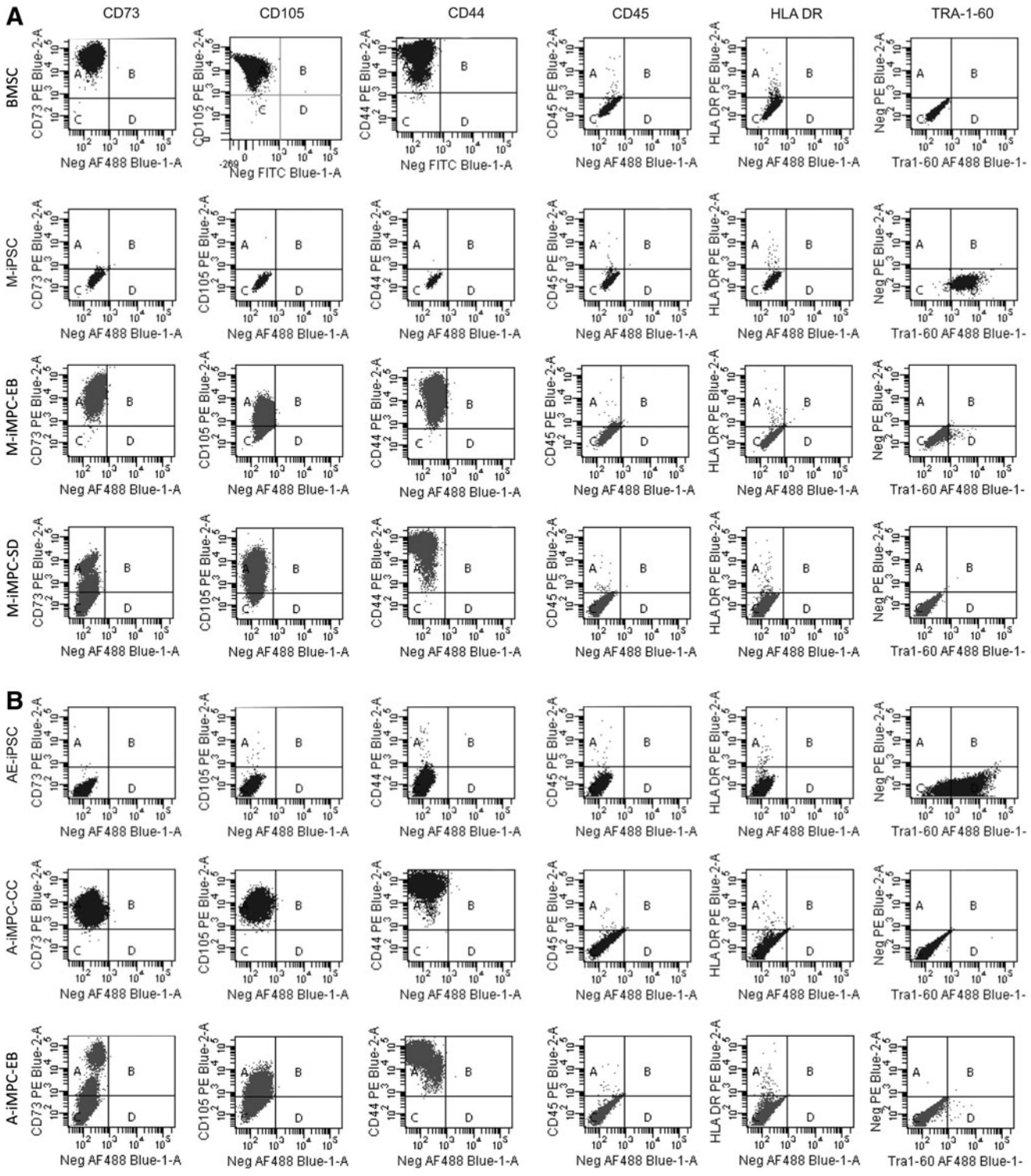

FIG. 3. Flow cytometric analysis of surface marker expression in M-iMPC-EBs and M-iMPC-SDs **(A)** as well as A-iMPC-CCs and A-iMPC-EBs **(B)** in comparison to BMSCs and iPSCs. Assessed surface markers included those typically present on BMSCs (CD73, CD105, and CD44), typically absent on BMSCs (CD45, HLA DR), and associated with pluripotency (TRA-1-60). Analysis of iMPC surface markers was performed with pools of four to six replicate cell lines.

Pluripotency-associated genes *POU5F1* = *OCT3/4*, *PROM1* = *CD133*, *SOX2*, and *ZFP42* = *REX1* (Fig. 4B) were strongly expressed on iPSCs, but were very low in both BMSCs and iMPCs. Typical mesenchymal genes such as ACTA2 (α-smooth muscle actin), *ANPEP* = *CD13*, *CD44*, *COL1A1*, *ENG* = *CD105*, *NT5E* = *CD73*, *PDGFRB*, *RUNX2*, and *VIM* = Vimentin, on the other hand, were robustly expressed in BMSCs and were also present in iMPCs but not in iPSCs from which they were derived. Levels of these mesenchymal genes in iMPCs, while variable, were in the same range as in the

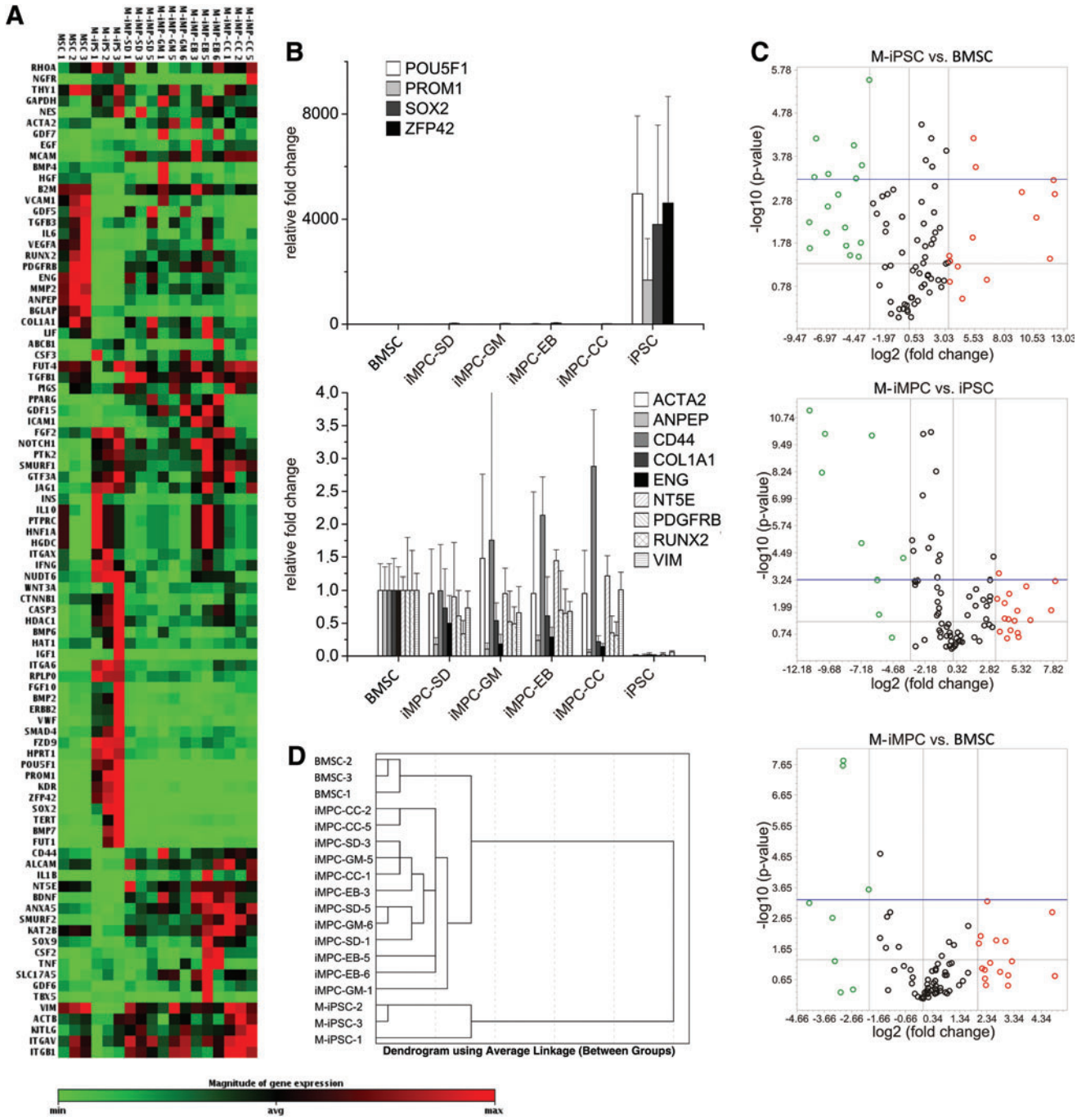

FIG. 4. Mesenchymal gene expression in M-iMPCs compared with BMSCs and M-iPSCs. **(A)** Heat map of PCR array results for each of the three BMSC, M-iPSC, and M-iMPC-SD, -EB, -CC, and GM replicates. **(B)** Expression of selected pluriptency-associated genes (*top*) and MSC-associated genes (*bottom*) by BMSCs, iPSCs, and iMPCs. Values are the mean of three replicates, and error bars represent 95% confidence intervals. **(C)** Volcano plots of differentially expressed genes between M-iPSCs and BMSCs (*top*), M-iMPCs and M-iPSCs (*middle*), as well as M-iMPCs and BMSCs (*bottom*). Genes with a >10-fold change (>4-fold for iMPC vs. BMSC) are colored *red* (over-expressed) and *green* (under-expressed). The *vertical gray lines* represent $P=0.05$, and the *vertical blue lines* represent significance at the Bonferroni-adjusted P value ($P<5.6\times10^{-4}$). Fold changes and P values of the individual genes are itemized in Table 2. All 12 iMPC lines that were investigated in the PCR array were grouped together ($n=12$) for this analysis. **(D)** Hierarchical cluster analysis (Pearson) of the average linkage between groups. MSC, mesenchymal stem cell. Color images available online at www.liebertpub.com/scd

parental MSCs. iMPCs were, therefore, obviously no longer iPSCs, but have instead become MSC-like.

A direct comparison analysis of the reprogrammed M-iPSC line with the parental BMSCs identified a total of 31 out of 84 genes of interest that were more than 10-fold differentially expressed, among which 9 reached statistical significance after Bonferroni correction: *ANPEP*, *ENG*, *HGF*, *MMP2*, *NT5E*, *VIM*, and *B2M* were expressed at significantly higher levels in BMSCs versus iPSCs; whereas *ITGA6* and *NGFR* were expressed at significantly higher levels in iPSCs (Table 2 and Fig. 4C top). As anticipated, the most strongly differentially regulated genes included pluripotency-associated genes (*ITGA6* [≈ 40-fold], *OCT3/4* [≈ 5,000-fold], *CD133* [≈ 1,700-fold], *SOX2* [≈ 3,800-fold], and *REX1* [≈ 4,600-fold]) that were strongly expressed in iPSCs. Typical mesenchymal markers, on the other hand, including (*CD13* [≈ 250-fold], *CD44* [≈ 100-fold], *COL1A1* [≈ 40-fold], *CD105* [≈ 100-fold], *CD73* [≈ 230-fold], *PDGFRB* [≈ 40-fold], *RUNX2* [≈ 125-fold], and *VIM* [≈ 16-fold]), were down-regulated in iPSCs.

When all 12 tested M-iMPC lines (3 replicate lines for each of the four derivation methods EB, SD, CC, and GM) were grouped together and compared with the parental M-iPSCs, the identity of the differentially expressed genes largely overlapped with those in BMSCs (Table 2 and Fig. 4C middle). Pluripotency markers [*OCT3/4* (≈ 1,000-fold), *CD133* (≈ 1,200-fold), *SOX2* (≈ 140-fold), and *REX1* (≈ 2,400-fold)] were strongly down-regulated in M-iMPCs versus M-iPSCs, while genes associated with MSCs [*CD13* (≈ 30-fold), *CD44* (≈ 200-fold), *CD73* (≈ 250-fold), *CD105* (≈ 30-fold), *COL1A1* (≈ 20-fold), *PDGFRB* (≈ 20-fold), *RUNX2* (≈ 50-fold), and *VIM* (≈ 10-fold)] tended to be up-regulated. However, a direct comparison of iMPCs ($n = 12$) versus BMSCs (Table 2 and Fig. 4C bottom) still showed that not all genes which were regulated after reprogramming to iPSCs reverted completely to levels measured in BMSCs. Interestingly, three genes highly active in BMSCs [*BGLAP* (≈ 8-fold), *CD13* (≈ 8-fold), and *CD105* (≈ 4-fold)] were expressed at significantly lower levels in all iMPCs, irrespective of the derivation method (Table 2). Lower *CD105* gene expression confirmed our flow cytometry data on *CD105* that tended to be lower in iMPCs than in BMSCs. The observed heterogeneous expression of *CD73* (*NT5E*) that showed lower protein levels for iMPCs than for BMSCs was, however, not reflected at the mRNA level. Taken together, gene expression of iMPCs was not completely identical

Table 2. Comparative Analysis of Gene Expression Profiles of M-iPSCs, BMSCs, and M-iMPCs

M-iPSCs vs. BMSCs			*M-iMPCs vs. iPSCs*			*M-iMPCs vs. BMSCs*		
	Fold regulation	P *value*		*Fold regulation*	P *value*		*Fold regulation*	P *value*
ACTA2	−63.215	0.001264	ACTA2	67.2736	0.043619	ANPEP	−7.7852	0
ANPEP	−255.0534	0.000503	ALCAM	11.0968	0.004402	BGLAP	−7.7891	0
CD44	−114.4709	0.002402	ANPEP	32.7615	0.016059	BMP4	−8.2732	0.580941
COL1A1	−42.2736	0.007278	BDNF	16.2923	0.006901	ENG	−4.0223	0.000258
ENG	−111.8829	0.000429	CD44	207.207	0.015496	GDF5	−9.5773	0.058074
GDF5	−338.1099	0.022303	COL1A1	20.2052	0.040322	HGF	−6.0178	0.469051
GDF6	−16.8462	0.016455	ENG	27.8156	0.046611	IL6	−10.111	0.002207
HGF	−25.069	0.000093	GDF5	35.3032	0.270552	VCAM1	−18.5136	0.000729
IL6	−31.9214	0.032392	GDF6	22.4802	0.12643	ABCB1	8.7114	0.353566
LIF	−19.2235	0.034945	ICAM1	12.5828	0.148623	BDNF	6.4017	0.011868
MMP2	−22.5339	0.000541	IL1B	33.4407	0.17275	EGF	4.7882	0.109488
NT5E	−231.3767	0.000065	LIF	16.6949	0.036627	GDF15	4.4931	0.097873
PDGFRB	−39.4934	0.019346	NT5E	256.0413	0.000668	GDF7	4.9471	0.344188
RUNX2	−124.9395	0.009671	PDGFRB	20.9229	0.002621	ICAM1	7.0347	0.128943
VCAM1	−345.9559	0.005506	RUNX2	53.4906	0.001209	IL1B	28.73	0.175756
VIM	−15.9424	0.000267	VCAM1	18.6866	0.299739	ITGA6	8.1682	0.012987
B2M	−10.4453	0.000003	VIM	12.0833	0.0003	KDR	8.6601	0.163664
ABCB1	40.6224	0.01257	BMP7	−60.2573	0.000591	MCAM	5.1046	0.000647
BMP2	10.4339	0.033386	IGF1	−55.4414	0.024046	NES	5.5138	0.064289
BMP7	93.1006	0.118691	KDR	−81.2145	0	NOTCH1	4.3219	0.008615
FUT1	10.5677	0.130586	NGFR	−26.9519	0.273615	POU5F1	4.8301	0.211454
IGF1	22.3993	0.328311	POU5F1	−1027.9075	0	PPARG	9.606	0.056885
ITGA6	42.3272	0.000062	PROM1	−1215.4641	0	SMURF2	4.1398	0.015032
KDR	703.3227	0.001109	SOX2	−141.9279	0.000012	SOX2	26.7393	0.001455
NES	11.0221	0.043474	VWF	−14.7141	0.00006			
NGFR	48.8618	0.000294	ZFP42	−2380.2596	0			
POU5F1	4964.9436	0.001245						
PROM1	1683.328	0.004369						
SOX2	3795.0555	0.039305						
VWF	17.0207	0.058848						
ZFP42	4609.4139	0.000587						

Up-regulated genes are in *red*, and down-regulated genes are in *green*. Nonsignificantly regulated genes ($P > 5.6 \times 10^{-4}$) are printed in *gray*.
iPSCs, induced pluripotent stem cells.
Color images available online at www.liebertpub.com/scd

among the four derivation methods, and each of the cell lines derived with specific methods tended to exhibit, to some extent, a unique gene expression profile (Supplementary Table S1).

A cluster analysis predictably grouped iPSCs as distinct from BMSCs (Fig. 4D). However, interestingly, iMPCs did not cluster together with BMSCs but rather as an intermediate group inbetween BMSCs and iPSCs. Moreover, iMPCs did not sub-cluster according to the respective generation method (EB, SD, CC, and GM) but rather as one large separate group. This finding suggests that random differences between replicate iMPC lines were more pronounced than potential differences caused by separate derivation methods.

General in vitro differentiation capability of iMPCs

Since PSC offsprings have been termed ''mesenchymal stem cells'' based on their expression of typical MSC surface markers and positive results of standard lineage analyses [13,33–35], we initially tested whether our iMPCs would also calcify their matrix under osteogenic conditions, form lipid droplets under adipogenic induction, and deposit sulfated proteoglycans under chondrogenic conditions. Noninduced controls did not stain positive in these analyses (Supplementary Fig. S4) [36]. Since for MSCs it is well known that high cellular activity accompanied by high proliferation rates is indicative of high differentiation capacity [37], we chose one M-iMPC line with a high proliferation rate (M-iMPC-GM3) for this pilot experiment. After 3 weeks of induction culture, Alizarin Red staining verified matrix mineralization in osteogenic conditions (Supplementary Fig. S5), Oil Red O staining detected formation of intracellular lipid vesicles, and Alcian blue staining confirmed proteoglycan deposition in monolayer culture. In these preliminary experiments, iMPCs performed as well as BMSCs that were tested in parallel. Our iMPCs, therefore, clearly exhibit mesenchymal-like characteristics similar to previous studies [13,33–35].

Histological evaluation of the quality of iMPC differentiation potential in comparison with BMSCs

To further test whether iMPCs possessed the differentiation efficiency and characteristics of BMSCs, we investigated the performance of all our iMPC lines under standard BMSC differentiation conditions in direct comparison with the parental BMSCs. Similar to what our preliminary experiment had suggested, iMPCs were capable of strong matrix mineralization detected with Alizarin Red (Fig. 5A, B). However, while reproducible levels were seen in BMSCs, Alizarin Red staining was substantially variable in replicate iMPC lines.

After 3 weeks in adipogenic medium, BMSCs gave rise to cells containing large lipid vesicles stained with Oil Red O (Fig. 5C). For BMSCs from this particular donor, lipid droplets were detected in $< 50\%$ of the cells. In comparison, after 3 weeks in adipogenic culture, iMPCs again exhibited very heterogeneous differentiation outcomes (Fig. 5C). Some cell lines formed lipid vesicles in all cells, while others did not appear to be adipogenically induced. The main difference between adipogenically induced BMSCs and iMPCs was that lipid vesicles stayed small in size in the latter. Dye solubilization and quantitation showed significantly higher levels of dye incorporation in BMSCs compared with all iMPC lines with one exception (Fig. 5D). M-iMPC-SDs that had been generated via spontaneous differentiation reached dye incorporation values comparable to BMSCs.

Chondrogenic differentiation of BMSCs performed in standard micromass pellet culture resulted in robust and reproducible production of cartilaginous ECM [rich in sGAGs and COL2A1 (Fig. 5E)]. In contrast, GAG deposition by iMPCs according to Alcian blue staining was very low and rarely accompanied by collagen II deposition. In line with histological staining results, sGAG quantification resulted in significantly reduced sGAG levels in all iMPC lines compared with BMSCs (Fig. 5F).

Gene expression in differentiated iMPCs compared to BMSCs

To further evaluate the differentiation capacity of iMPCs, we quantified lineage-specific gene expression. Under osteogenic conditions, BMSCs expressed *COL1A1*, *BGLAP* (osteocalcin), and *IBSP* (Fig. 6A–C). IMPCs also expressed *COL1A1* at similar levels as BMSCs, but *BGLAP* and *IBSP* remained low. Similar results were obtained for *ALP* gene expression and enzyme activity (Supplementary Fig. S6). Matrix mineralization according to Alizarin Red staining, therefore, did not correlate with osteogenic marker expression, suggesting that, consistent with previous studies [38], matrix calcification was not necessarily a specific parameter for osteogenesis. These results showed that in contrast to BMSCs, dexamethasone in combination with ascorbic acid and β-glycerophosphate was not sufficient to effectively induce iMPC osteogenesis.

After 3 weeks in adipogenic conditions, common adipogenic lineage markers were robustly expressed in BMSCs (Fig. 6D–F). In iMPCs, *PPARG* and *aP2* were also detected but remained at lower levels in most iMPC lines than in BMSCs. *LPL* was rarely induced in iMPCs. Dexamethasone and isobutylmethylxanthine that are potent inducers for BMSC adipogenesis were, therefore, less effective for iMPCs.

Under chondrogenic conditions, BMSCs robustly expressed *COL2A1*, *ACAN*, and *COMP* at 3 weeks of induction (Fig. 6G–I). In iMPCs, *COL2A1* and *ACAN* remained at minimal levels. Only *COMP* was robustly expressed in iMPCs but at significantly lower levels than in BMSCs. These results, therefore, showed that TGF-β was less effective in inducing iPMC chondrogenesis, compared with BMSCs.

Discussion

MSC-like derivatives from PSCs have recently gained increasing attention. PSCs as a new source for MSCs could potentially overcome the persisting limited supply of cells that are required in large quantities for regenerative therapeutic applications. MSC-like PSC offsprings have often been termed ''MSCs'' [10,39] on the basis of experiments showing that these PSC derivatives satisfied the minimal MSC criteria put forth by the ISCT [22,23]. On the other hand, recent published studies based on gene expression data [10,15,40] and in vitro differentiation assays [29,39,41–43]

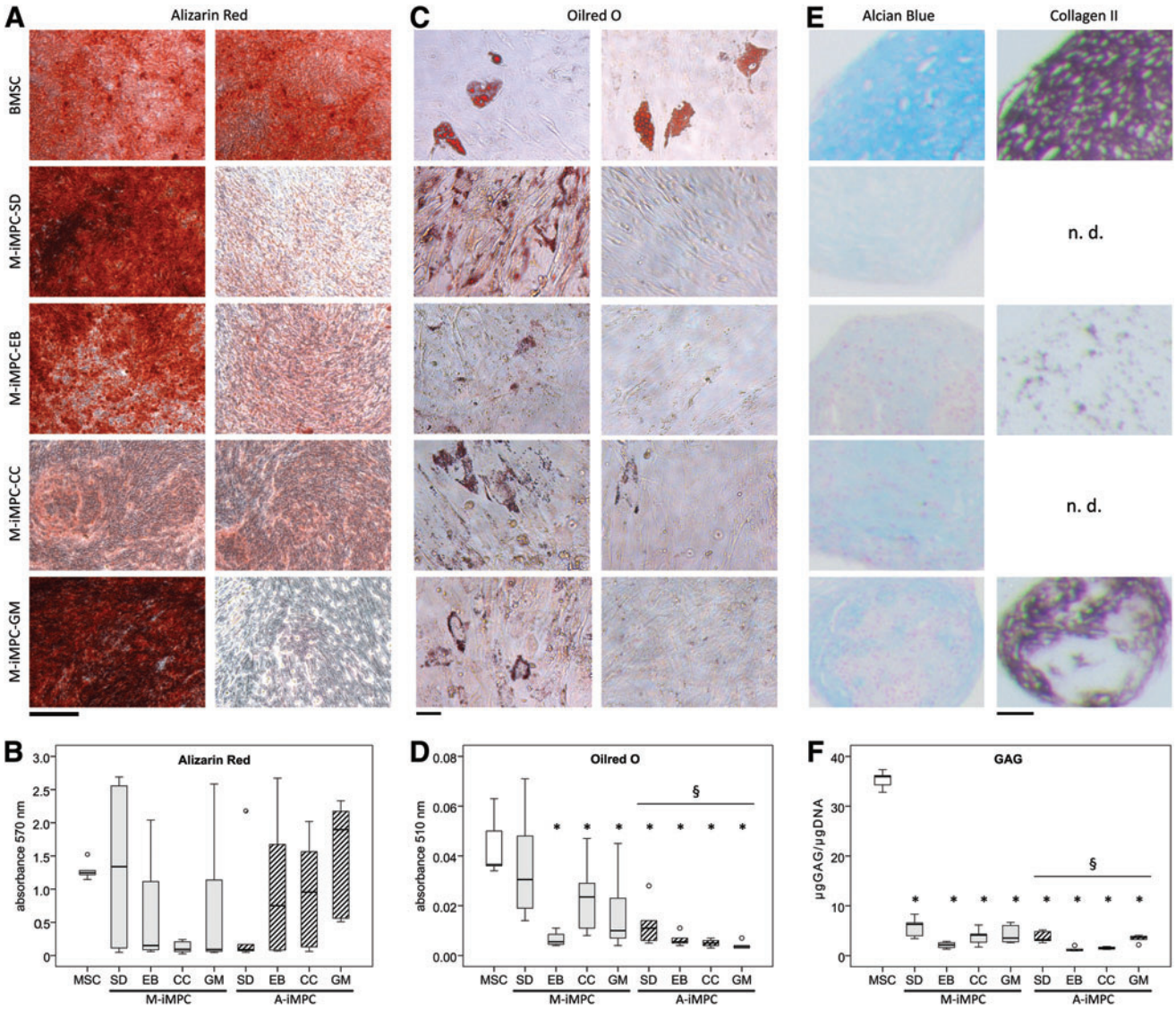

FIG. 5. Quality of in vitro trilineage differentiation capacity of iMPCs assessed via histological staining. **(A)** Alizarin Red staining of matrix calcification in BMSCs and M-iMPCs after 3 weeks under osteogenic conditions. Best and worst results are shown for each derivation method. **(B)** Quantitative analysis of Alizarin Red incorporation for BMSCs versus M-iMPCs and A-iMPCs. **(C)** Best and worst results of Oil Red O staining of lipid vesicles after 3 weeks in adipogenic medium for BMSCs and M-iMPCs. **(D)** Quantitative analysis of dye incorporation for BMSCs versus M-iMPCs and A-iMPCs. **(E)** Alcian blue staining of sGAG deposition (*left*) and collagen type II immunostaining (*right*) of BMSCs and M-iMPCs after 3 weeks in chondrogenic pellet culture. Best results are shown for M-iMPCs. **(F)** Quantitative sGAG assay of chondrogenic BMSC, M-iMPC, and A-iMPC pellets. Scale bars: 100 µm for **(A)**; 50 µm for **(C, E)**. Median values are presented (bars), with the boxes representing first and third quartile and whiskers representing maximal and minimal values. Outliers are depicted as *circles*. Group sizes were $n=3$ for BMSCs (independent replicates from one donor) and $n=4$–6 for iMPCs (replicate cell lines). Significant differences ($P<0.05$) between iMPCs and BMSCs are designated by an *asterisk*. Significant differences ($P<0.05$) between M-iMPCs and A-iMPCs are designated by §. sGAG, sulfated glycosaminoglycan. Color images available online at www.liebertpub.com/scd

suggested differences between BMSCs and MSC-like PSC derivatives. However, when interpreting these studies, it should be taken into consideration that the MSCs and ESCs originated from different donors. Therefore, it could not be ruled out that the well-recognized BMSC donor dependency contributed to the observed differences. We, thus, designed our study to specifically circumvent the donor variability issue by using a single source of human BMSCs for reprogramming to generate the stable M-iPSC line that was subsequently differentiated into the mesenchymal lineage. The mesenchymal offsprings (iMPCs) were then directly compared with BMSCs from the same donor and batch that had been used for reprogramming.

In agreement with previous studies [44,45], our results confirmed that iMPCs exhibited an MSC-like morphology, expressed MSC-associated surface markers, and mesenchymal genes, while pluripotency-associated genes were strongly down-regulated. Moreover, they were capable of a limited in

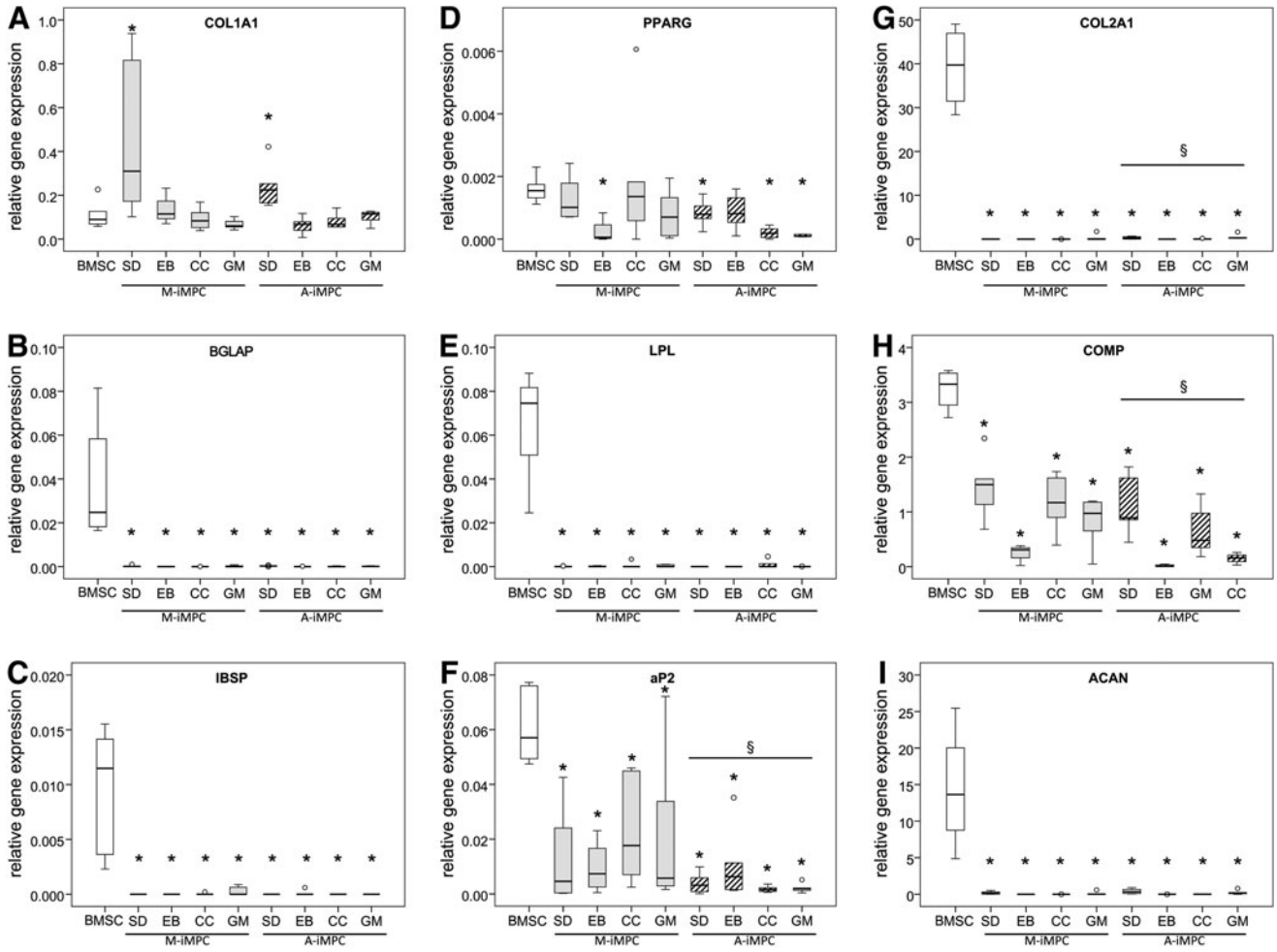

FIG. 6. Quantitative gene expression rates of osteogenic **(A–C)**, adipogenic **(D–F)**, and chondrogenic **(G–I)** lineage markers. Gene abbreviations are according to NCBI gene database. Values are median (*bars*), with the boxes representing first and third quartile and whiskers representing maximal and minimal values. Outliers (1.5 to 3-fold IQR) are depicted as *circles*. Group sizes were $n=3$ for BMSCs (independent replicates from one donor) and $n=4$–6 for iMPCs (replicate cell lines). Significant differences ($P<0.05$) between iMPCs and BMSCs are designated by an *asterisk*. Significant differences ($P<0.05$) between M-iMPCs and A-iMPCs are designated by §.

vitro trilineage differentiation and are, therefore, MSC-like cells. However, the direct side-by-side comparison between iMPCs and the original BMSCs revealed significant differences, especially at the gene expression level with regard to inducibility to undergo trilineage differentiation in vitro, where BMSCs generally out-performed iMPCs. This specific comparison of iMPCs with their parental BMSCs was the only way to detect these differences, and our data, therefore, for the first time strongly indicate that despite their apparent resemblance to BMSCs, iMPCs represent a discrete cell population and are not identical to primary BMSCs. This suggests that at least for PMPCs, compliance with the ISCT criteria, which was originally developed to distinguish BMSCs from hematopoietic stem cells in bone marrow preparations, may not be sufficient to verify successful derivation of MSCs from PSCs. Indeed, MSC-associated surface markers are known to be also expressed on non-MSCs, for example, fibroblasts (recently reviewed by Boxall and Jones [46]), and even in vitro trilineage induction is prone to misinterpretation [47]. In our opinion, a careful comparison with high-performing primary BMSCs, ideally from the same donor, is essential to establish the biological fidelity of PSC-derived MSCs. Importantly, successful histological staining results after in vitro induction also needs to be interpreted with care. Naturally, in vivo assessment would be even more preferable.

It should be noted that in our study design, BMSCs from only one donor were used, and it is, thus, not possible to assess potential donor-dependent differences in the capacity of iMPCs to regain an MSC-like phenotype. In addition, we chose a high-performing, parental BMSC population with optimal performance in trilineage in vitro differentiation assays. While a lower performing BMSC parent might yield iMPCs that are more similar, we specifically intended to set the standard high in order to ultimately test the functional capabilities of iMPCs.

Weak in vitro differentiation outcomes in our study do not necessarily indicate low iMPC differentiation capacity. The focus of our study was the direct comparison of iMPCs with BMSCs, and we did not investigate whether additional growth factors or culture conditions might be able to more

efficiently induce iMPC differentiation in vitro. However, we performed a preliminary test of ectopic in vivo bone formation (Supplementary Data and Supplementary Fig. S7) and observed that the derived iMPCs were, indeed, able to exhibit BMP2-induced osteogenic activity in vivo, and are, thus, MSC-like. Additional experiments will need to be carried out in order to compare the bone regeneration capacity of iMPCs with MSCs.

Since ready mesenchymal differentiation of a BMSC-derived iPSC line might possibly be related to epigenetic memory, we also used an iPSC line derived from human amniotic epithelium (AE-iPSCs [28]) as control. Overall, the difference between A-iMPCs and M-iMPCs, although statistically significant for some differentiation markers, was generally very low. This indicated that epigenetic memory in our study had only a minor influence on mesenchymal differentiation of iPSCs. Likewise, Nasu et al. recently reported that clonal differences exerted a more pronounced influence on the lineage-specific differentiation propensity of human iPSCs than tissue origin [48].

Particularly striking in our study was the high iMPC heterogeneity that was not only noticeable for cell morphology and surface marker expression but also caused high variability in differentiation in vitro. While we did not further investigate what caused iMPC heterogeneity, we speculate that heterogeneity might be a consequence of the applied iMPC derivation strategies, all of which were based on spontaneous differentiation. Indeed, our comparison of iMPC lines derived by the three most commonly used strategies (ie, EB outgrowth, spontaneous differentiation of colonies, or coculture with MSCs) suggested no significant differences between cell lines derived via any one of these methods. This is consistent with the previously mentioned study by Barbet et al. [10], who did not report any specific differences between two essentially different PMPC lines (spontaneous differentiation in serum-containing medium vs. EB outgrowth culture). Even coculture with feeder MSCs that provide growth factors and trophic molecules which could potentially induce specific cellular signaling pathways and direct a guided differentiation process yielded iMPCs highly similar to the cells derived by spontaneous differentiation. The shift to serum-containing medium as well as reduced/discontinued FGF-2 and TGF-β supply obviously outweighed the effects of the additional cytokines provided by the MSC-conditioned medium.

Although further studies are obviously needed to characterize the iMPC subpopulations, we hypothesize that within our mixed cultures, progenitor cells with true MSC capacity spontaneously emerged and that differentiation outcomes were dependent on the frequency of such progenitor cells in individual iMPC lines. Naturally, it would be interesting to enrich our heterogeneous populations for multipotent progenitor cells, but such attempts are currently limited, as MSCs do not have exclusive markers. Alternatively, sophisticated strategies could be considered in order to selectively direct guided iPSC differentiation into MSCs in contrast to inducing spontaneous events. Indeed, in related fields of research, recent approaches to enhance the efficiency of in vitro guided PSC differentiation have attempted to recapitulate the regulatory pathways that control the establishment of the respective lineage in the early embryo [49–51]. It would be interesting to investigate whether such an approach to temporally vary cytokine cocktails to direct a multi-stage differentiation process resembling embryonic development could successfully induce PSCs to differentiate into genuine MSCs and whether such cells would comply with the most stringent stem cell criteria (self-renewal and multipotency). On the other hand, such approaches are highly laborious and costly, and simple strategies might still be preferable, albeit confounded by inherent heterogeneity, when they give rise to cells that are attractive for regenerative applications. Indeed, in agreement with our results, several groups have reported successful in vivo bone formation of PSCs that were preinduced into MSC-like cells [39,52]. Moreover, current debate has focused on whether the regenerative activity of MSCs might actually be attributable to their trophic and immune modulatory activity that enable them to attract host cells and regulate tissue regeneration by host cells rather than their capacity to differentiate. Interestingly, there is already preliminary evidence that PMPCs might also exhibit such activities [33,53].

Taken together, the use of PMPCs needs to be carefully considered in the context of our findings that they are not identical to MSCs. Nevertheless, their potentially unlimited availability still makes them highly attractive, particularly in view of the promising preliminary in vivo data.

Conclusions

In accordance with previous reports on ESCs, our data on iPSCs strongly suggest that MSC-like progenitor cells generated from PSCs via spontaneous differentiation are not identical to primary BMSCs. However, MSC-like iMPCs are obviously a distinct cell population. On this basis, we recommend distinguishing MSCs from PSC-derived MSC-like progenitors and suggest the terms EMPC and iMPC (or PMPCs for both), respectively, for cells derived from ESCs and iPSCs, respectively [31,54].

Since specific iMPC quality and general characteristics were not markedly dependent on the derivation method, the most cost- and time-effective as well as experimentally easiest method would be favored for regenerative applications. Thus, direct treatment of PSC cultures with serum-containing media or with chemically defined media supplemented with appropriate cytokines, or even EB outgrowth cultures might be preferable compared with coculture with mouse or human cell lines.

Directing PMPCs into lineage-specific differentiation and generating tissue constructs that are applicable for regenerative medicine calls for more sophisticated approaches than those currently used for MSCs, but their general capacity to form various tissues has been shown [31,55]. Alternatively, more refined and effective methods could be developed to derive PSC offsprings that are more similar to MSCs. The true attractiveness of iMPCs for therapeutic application is that they can easily be derived in virtually unlimited amounts. Moreover, the somatic origin of iPSCs enables autologous cell derivation, thus avoiding the legal and ethical constraints associated with ESCs.

Acknowledgments

Reprogramming was performed at the University of Pittsburgh Stem Cell Core. AE-iPSCs were a kind gift of Gerald Schatten (University of Pittsburgh). Cytogenetic studies were carried out in the University of Pittsburgh

Cancer Institute Cell Culture and Cytogenetics Facility, supported in part by the University of Pittsburgh Cancer Institute. Animal studies were performed by the Transgenic and Molecular Core Facility at the Pittsburgh Magee Womens Research Institute. Flow cytometry was performed at the Flow Cytometry Facility of the McGowan Institute for Regenerative Medicine, the University of Pittsburgh. The authors also thank Paul Manner (University of Washington) for providing surgical specimens, Jian Tan for isolating MSCs and helping with histology, Jocelyn Danielle Mich-Basso for assisting with iPSCs and reprogramming, Ian Goodwin for helping with histology, Rachel Brick for test of differentiation strategies, as well as Bing Wang, Ying Tang, and Hang Lin for the in vivo implantation experiment. This study was supported in part by the German Research Foundation (Deutsche Forschungsgemeinschaft DFG, DI 1684/1-1), and funding from the Commonwealth of Pennsylvania Department of Health, the U.S. Department of Defense (W81XWH-08-2-0032), and the National Institutes of Health (1U18 TR000532).

Author Disclosure Statement

No competing financial interests exist.

References

1. Caplan AI and JE Dennis. (2006). Mesenchymal stem cells as trophic mediators. J Cell Biochem 98:1076–1084.
2. Nauta AJ and WE Fibbe. (2007). Immunomodulatory properties of mesenchymal stromal cells. Blood 110:3499–3506.
3. Bruder SP, N Jaiswal and SE Haynesworth. (1997). Growth kinetics, self-renewal, and the osteogenic potential of purified human mesenchymal stem cells during extensive subcultivation and following cryopreservation. J Cell Biochem 64:278–294.
4. Stolzing A, E Jones, D McGonagle and A Scutt. (2008). Age-related changes in human bone marrow-derived mesenchymal stem cells: consequences for cell therapies. Mech Ageing Dev 129:163–173.
5. Bieback K and I Brinkmann. (2010). Mesenchymal stromal cells from human perinatal tissues: from biology to cell therapy. World J Stem Cells 2:81–92.
6. Guillot PV, C Gotherstrom, J Chan, H Kurata and NM Fisk. (2007). Human first-trimester fetal MSC express pluripotency markers and grow faster and have longer telomeres than adult MSC. Stem Cells 25:646–654.
7. Wu SM and K Hochedlinger. (2011). Harnessing the potential of induced pluripotent stem cells for regenerative medicine. Nat Cell Biol 13:497–505.
8. Barberi T, LM Willis, ND Socci and L Studer. (2005). Derivation of multipotent mesenchymal precursors from human embryonic stem cells. PLoS Med 2:e161.
9. Lian Q, E Lye, K Suan Yeo, E Khia Way Tan, M Salto-Tellez, TM Liu, N Palanisamy, RM El Oakley, EH Lee, B Lim and SK Lim. (2007). Derivation of clinically compliant MSCs from CD105+, CD24- differentiated human ESCs. Stem Cells 25:425–436.
10. Barbet R, I Peiffer, A Hatzfeld, P Charbord and JA Hatzfeld. (2011). Comparison of gene expression in human embryonic stem cells, hESC-derived mesenchymal stem cells and human mesenchymal stem cells. Stem Cells Int 2011:368192.
11. Lee EJ, HN Lee, HJ Kang, KH Kim, J Hur, HJ Cho, J Lee, HM Chung, J Cho, et al. (2010). Novel embryoid body-based method to derive mesenchymal stem cells from human embryonic stem cells. Tissue Eng Part A 16:705–715.
12. Karlsson C, K Emanuelsson, F Wessberg, K Kajic, MZ Axell, PS Eriksson, A Lindahl, J Hyllner and R Strehl. (2009). Human embryonic stem cell-derived mesenchymal progenitors—potential in regenerative medicine. Stem Cell Res 3:39–50.
13. Trivedi P and P Hematti. (2007). Simultaneous generation of CD34+ primitive hematopoietic cells and CD73+ mesenchymal stem cells from human embryonic stem cells cocultured with murine OP9 stromal cells. Exp Hematol 35:146–154.
14. Hwang NS, S Varghese, HJ Lee, Z Zhang, Z Ye, J Bae, L Cheng and J Elisseeff. (2008). *In vivo* commitment and functional tissue regeneration using human embryonic stem cell-derived mesenchymal cells. Proc Natl Acad Sci U S A 105:20641–20646.
15. de Peppo GM, S Svensson, M Lenneras, J Synnergren, J Stenberg, R Strehl, J Hyllner, P Thomsen and C Karlsson. (2010). Human embryonic mesodermal progenitors highly resemble human mesenchymal stem cells and display high potential for tissue engineering applications. Tissue Eng Part A 16:2161–2182.
16. Olivier EN and EE Bouhassira. (2011). Differentiation of human embryonic stem cells into mesenchymal stem cells by the ''raclure'' method. Methods Mol Biol 690: 183–193.
17. Trivedi P and P Hematti. (2008). Derivation and immunological characterization of mesenchymal stromal cells from human embryonic stem cells. Exp Hematol 36:350–359.
18. Phinney DG, G Kopen, W Righter, S Webster, N Tremain and DJ Prockop. (1999). Donor variation in the growth properties and osteogenic potential of human marrow stromal cells. J Cell Biochem 75:424–436.
19. Pevsner-Fischer M, S Levin and D Zipori. (2011). The origins of mesenchymal stromal cell heterogeneity. Stem Cell Rev 7:560–568.
20. Deyle DR, IF Khan, G Ren, PR Wang, J Kho, U Schwarze and DW Russell. (2012). Normal collagen and bone production by gene-targeted human osteogenesis imperfecta iPSCs. Mol Ther 20:204–213.
21. Kuznetsov SA, N Cherman and PG Robey. (2011). *In vivo* bone formation by progeny of human embryonic stem cells. Stem Cells Dev 20:269–287.
22. Dominici M, K Le Blanc, I Mueller, I Slaper-Cortenbach, F Marini, D Krause, R Deans, A Keating, D Prockop and E Horwitz. (2006). Minimal criteria for defining multipotent mesenchymal stromal cells. The International Society for Cellular Therapy position statement. Cytotherapy 8:315–317.
23. Bourin P, BA Bunnell, L Casteilla, M Dominici, AJ Katz, KL March, H Redl, JP Rubin, K Yoshimura and JM Gimble. (2013). Stromal cells from the adipose tissue-derived stromal vascular fraction and culture expanded adipose tissue-derived stromal/stem cells: a joint statement of the International Federation for Adipose Therapeutics (IFATS) and Science and the International Society for Cellular Therapy (ISCT). Cytotherapy 15:641–648.
24. Yagi H, J Tan and RS Tuan. (2012). Polyphenols suppress hydrogen peroxide-induced oxidative stress in human

bone-marrow derived mesenchymal stem cells. J Cell Biochem 114:1163–1173.
25. Caterson EJ, LJ Nesti, KG Danielson and RS Tuan. (2002). Human marrow-derived mesenchymal progenitor cells: isolation, culture expansion, and analysis of differentiation. Mol Biotechnol 20:245–256.
26. Lin B, J Kim, Y Li, H Pan, X Carvajal-Vergara, G Salama, T Cheng, Y Li, CW Lo and L Yang. (2012). High-purity enrichment of functional cardiovascular cells from human iPS cells. Cardiovasc Res 95:327–335.
27. Takahashi K, K Tanabe, M Ohnuki, M Narita, T Ichisaka, K Tomoda and S Yamanaka. (2007). Induction of pluripotent stem cells from adult human fibroblasts by defined factors. Cell 131:861–872.
28. Momcilovic O, L Knobloch, J Fornsaglio, S Varum, C Easley and G Schatten. (2010). DNA damage responses in human induced pluripotent stem cells and embryonic stem cells. PLoS One 5:e13410.
29. Teramura T, Y Onodera, T Mihara, Y Hosoi, C Hamanishi and K Fukuda. (2010). Induction of mesenchymal progenitor cells with chondrogenic property from mouse-induced pluripotent stem cells. Cell Reprogram 12:249–261.
30. Lin H, G Yang, J Tan and RS Tuan. (2012). Influence of decellularized matrix derived from human mesenchymal stem cells on their proliferation, migration and multi-lineage differentiation potential. Biomaterials 33:4480–4489.
31. Marolt D, IM Campos, S Bhumiratana, A Koren, P Petridis, G Zhang, PF Spitalnik, WL Grayson and G Vunjak-Novakovic. (2012). Engineering bone tissue from human embryonic stem cells. Proc Natl Acad Sci U S A 109:8705–8709.
32. Takahashi K and S Yamanaka. (2006). Induction of pluripotent stem cells from mouse embryonic and adult fibroblast cultures by defined factors. Cell 126:663–676.
33. Sanchez L, I Gutierrez-Aranda, G Ligero, R Rubio, M Munoz-Lopez, JL Garcia-Perez, V Ramos, PJ Real, C Bueno, et al. (2011). Enrichment of human ESC-derived multipotent mesenchymal stem cells with immunosuppressive and anti-inflammatory properties capable to protect against experimental inflammatory bowel disease. Stem Cells 29:251–262.
34. Lian Q, Y Zhang, J Zhang, HK Zhang, X Wu, FF Lam, S Kang, JC Xia, WH Lai, et al. (2010). Functional mesenchymal stem cells derived from human induced pluripotent stem cells attenuate limb ischemia in mice. Circulation 121:1113–1123.
35. Olivier EN, AC Rybicki and EE Bouhassira. (2006). Differentiation of human embryonic stem cells into bipotent mesenchymal stem cells. Stem Cells 24:1914–1922.
36. Diederichs S, K Baral, M Tanner and W Richter. (2012). Interplay between local versus soluble transforming growth factor-beta and fibrin scaffolds: role of cells and impact on human mesenchymal stem cell chondrogenesis. Tissue Eng Part A 18:1140–1150.
37. Janicki P, S Boeuf, E Steck, M Egermann, P Kasten and W Richter. (2011). Prediction of *in vivo* bone forming potency of bone marrow-derived human mesenchymal stem cells. Eur Cell Mater 21:488–507.
38. Evans ND, RJ Swain, E Gentleman, MM Gentleman and MM Stevens. (2012). Gene-expression analysis reveals that embryonic stem cells cultured under osteogenic conditions produce mineral non-specifically compared to marrow stromal cells or osteoblasts. Eur Cell Mater 24:211–223.
39. Arpornmaeklong P, SE Brown, Z Wang and PH Krebsbach. (2009). Phenotypic characterization, osteoblastic differentiation, and bone regeneration capacity of human embryonic stem cell-derived mesenchymal stem cells. Stem Cells Dev 18:955–968.
40. Yen ML, CH Hou, KY Peng, PC Tseng, SS Jiang, CT Shun, YC Chen and ML Kuo. (2011). Efficient derivation and concise gene expression profiling of human embryonic stem cell-derived mesenchymal progenitors (EMPs). Cell Transplant 20:1529–1545.
41. Domev H, M Amit, I Laevsky, A Dar and J Itskovitz-Eldor. (2012). Efficient engineering of vascularized ectopic bone from human embryonic stem cell-derived mesenchymal stem cells. Tissue Eng Part A 18:2290–2302.
42. Chen YS, RA Pelekanos, RL Ellis, R Horne, EJ Wolvetang and NM Fisk. (2012). Small molecule mesengenic induction of human induced pluripotent stem cells to generate mesenchymal stem/stromal cells. Stem Cells Transl Med 1:83–95.
43. Lee EJ, HJ Kang, HN Lee, SK Kang, KH Kim, SW Lee, G Lee, YB Park and HS Kim. (2012). New culture system for human embryonic stem cells: autologous mesenchymal stem cell feeder without exogenous fibroblast growth factor 2. Differentiation 83:92–100.
44. Varga N, Z Vereb, E Rajnavolgyi, K Nemet, F Uher, B Sarkadi and A Apati. (2011). Mesenchymal stem cell like (MSCl) cells generated from human embryonic stem cells support pluripotent cell growth. Biochem Biophys Res Commun 414:474–480.
45. Villa-Diaz LG, SE Brown, Y Liu, AM Ross, J Lahann, JM Parent and PH Krebsbach. (2012). Derivation of mesenchymal stem cells from human induced pluripotent stem cells cultured on synthetic substrates. Stem Cells 30:1174–1181.
46. Boxall SA and E Jones. (2012). Markers for characterization of bone marrow multipotential stromal cells. Stem Cells Int 2012:975871.
47. Fujita H, M Yamamoto, T Ogino, H Kobuchi, N Ohmoto, E Aoyama, T Oka, T Nakanishi, K Inoue and J Sasaki. (2013). Necrotic and apoptotic cells serve as nuclei for calcification on osteoblastic differentiation of human mesenchymal stem cells *in vitro*. Cell Biochem Funct 32:77–86.
48. Nasu A, M Ikeya, T Yamamoto, A Watanabe, Y Jin, Y Matsumoto, K Hayakawa, N Amano, S Sato, et al. (2013). Genetically matched human iPS cells reveal that propensity for cartilage and bone differentiation differs with clones, not cell type of origin. PLoS One 8:e53771.
49. Yang SL, E Harnish, T Leeuw, U Dietz, E Batchelder, PS Wright, J Peppard, P August, C Volle-Challier, et al. (2012). Compound screening platform using human induced pluripotent stem cells to identify small molecules that promote chondrogenesis. Protein Cell 3:934–942.
50. Kattman SJ, AD Witty, M Gagliardi, NC Dubois, M Niapour, A Hotta, J Ellis and G Keller. (2011). Stage-specific optimization of activin/nodal and BMP signaling promotes cardiac differentiation of mouse and human pluripotent stem cell lines. Cell Stem Cell 8:228–240.
51. Nostro MC, X Cheng, GM Keller and P Gadue. (2008). Wnt, activin, and BMP signaling regulate distinct stages in the developmental pathway from embryonic stem cells to blood. Cell Stem Cell 2:60–71.
52. Kuhn LT, Y Liu, NL Boyd, J Dennis, X Jiang, X Xin, L Charles, L Wang, HL Aguila, et al. (2013). Developmental-like bone regeneration by human embryonic stem cell-derived mesenchymal cells. Tissue Eng Part A 20:365–377.

53. Sze SK, DP de Kleijn, RC Lai, E Khia Way Tan, H Zhao, KS Yeo, TY Low, Q Lian, CN Lee, et al. (2007). Elucidating the secretion proteome of human embryonic stem cell-derived mesenchymal stem cells. Mol Cell Proteomics 6:1680–1689.
54. Evseenko D, Y Zhu, K Schenke-Layland, J Kuo, B Latour, S Ge, J Scholes, G Dravid, X Li, WR MacLellan and GM Crooks. (2010). Mapping the first stages of mesoderm commitment during differentiation of human embryonic stem cells. Proc Natl Acad Sci U S A 107:13742–13747.
55. Umeda K, J Zhao, P Simmons, E Stanley, A Elefanty and N Nakayama. (2012). Human chondrogenic paraxial mesoderm, directed specification and prospective isolation from pluripotent stem cells. Sci Rep 2:455.

Address correspondence to:
Rocky S. Tuan, PhD
Department of Orthopaedic Surgery
Center for Cellular and Molecular Engineering
University of Pittsburgh School of Medicine
450 Technology Drive, Room 221
Pittsburgh, PA 15219

E-mail: rst13@pitt.edu

Received for publication October 1, 2013
Accepted after revision March 13, 2014
Prepublished on Liebert Instant Online March 13, 2014